TITLE: Neural crest-like stem cell transcriptome analysis identifies LPAR1 in melanoma progression and therapy resistance.

AUTHORS: Jianglan Liu*[1], Vito W. Rebecca[*1.2], Andrew V. Kossenkov[1], Thomas Connelly[1], Qin Liu[1], Alexis Gutierrez[1], Min Xiao[1], Ling Li[1], Gao Zhang[1], Anastasia Samarkina[1], Delaine Zayasbazan[1], Jie Zhang[3], Chaoran Cheng[3], Zhi Wei[3], Gretchen M. Alicea[1], Mizuho Fukunaga-Kalabis[1], Clemens Krepler[1], Pedro Aza-Blanc[4], Chih-Cheng Yang[4], Bela Delvadia[1], Cynthia Tong[1], Ye Huang[1], Maya Delvadia[1], Alice S. Morais[1], Katrin Sproesser[1], Patricia Brafford[1], Joshua X. Wang[1], Marilda Beqiri[1], Rajasekharan Somasundaram[1+], Adina Vultur[1], Denitsa M. Hristova[1], Lawrence W. Wu[1], Yiling Lu[5], Gordon B. Mills[5], Wei Xu[6], Giorgos C. Karakousis[7], Xiaowei Xu[8], Lynn M. Schuchter[6], Tara C. Mitchell[6], Ravi K. Amaravadi[6], Lawrence N. Kwong[9], Dennie T. Frederick[10], Genevieve M. Boland[10], Joseph M. Salvino[1], David W. Speicher[1], Keith T. Flaherty[11.12], Ze'ev A. Ronai[4], Meenhard Herlyn[1#]

AFILLIATIONS:

1-Molecular and Cellular Oncogenesis Program and Melanoma Research Center, The Wistar Institute, Philadelphia, PA 19104, USA

2-Department of Biochemistry and Molecular Biology, Johns Hopkins Bloomberg School of Public Health, Baltimore, MD 21205, USA

3-Department of Computer Science, New Jersey Institute of Technology, Newark, NJ 07102, USA

4-Tumor Initiation and Maintenance Program, Cancer Center, Sanford Burnham Prebys Medical Discovery Institute, La Jolla, CA 92037, USA.

5-Department of Systems Biology, The University of Texas MD Anderson Cancer Center, Houston, TX 77030, USA

6-Abramson Cancer Center, Department of Medicine, Hospital of the University of Pennsylvania, University of Pennsylvania, Philadelphia, PA 19104, USA

7-Department of Surgery, Hospital of the University of Pennsylvania, Philadelphia, PA 19104, USA

8-Department of Pathology and Laboratory Medicine, Hospital of University of Pennsylvania, Philadelphia, PA 19104, USA

9-Department of Translational Molecular Pathology, The University of Texas MD Anderson Cancer

Center, Houston, TX 770303, USA

10-Division of Surgical Oncology, Massachusetts General Hospital Cancer Center, Boston, MA 02114, USA

11-Department of Medicine, Harvard Medical School, Boston, MA 02115, USA

12-Division of Medical Oncology, Massachusetts General Hospital Cancer Center, Boston, MA 02114, USA

* These authors contributed equally to this work.

+ Dr. Somasundaram passed away in February 2021, after the initial submission of this manuscript.

Corresponding author:

Meenhard Herlyn

The Wistar Institute

3601 Spruce Street

Philadelphia, PA 19104, USA

herlynm@wistar.org

(215) 898-3950

RUNNING TITLE: The stem cell LPAR1-axis drives therapy resistance in melanoma.

KEY WORDS: neural crest stem cells, melanoma, therapy resistance, LPAR1, YAP, mTOR

CONFLICT OF INTEREST STATEMENT: Gordon B. Mills serves as a consultant for AstraZeneca, Blend Therapeutics, Critical Outcome Technologies Inc., HanAl Bio Korea, Illumina, Nuevolution, Pfizer, Provista Diagnostics, Roche, SignalChem Lifesciences, Symphogen, Tau Therapeutics; owns stock in Catena Pharmaceuticals, PTV Healthcare Capital, Spindle Top Capital; and has received research funding from Adelson Medical Research Foundation, AstraZeneca, Critical Outcome Technologies Inc., GSK, and Illumina. Keith T. Flaherty has received consulting fees from GlaxoSmithKline (GSK), Roche, and Novartis. Meenhard Herlyn has received research support from GSK, BAYER, Plexxikon, MTargets and Actelion.

Funding: This work was supported by NIH grants R01 CA 182890, U54 CA224070, K01CA245124, the Dr. Miriam and Sheldon G. Adelson Medical Research Foundation and the Melanoma Research

Foundation. The support for Shared Resources utilized in this study was provided by Cancer Center Support Grant (CCSG) CA010815 to The Wistar Institute.

ABSTRACT (150 words)

Metastatic melanoma is challenging to clinically address. Although standard of care targeted therapy has high response rates in patients with BRAF-mutant melanoma, therapy relapse occurs in most cases. Intrinsically resistant melanoma cells drive therapy resistance and display molecular and biologic properties akin to neural crest-like stem cells (NCLSCs) including high invasiveness, plasticity and self-renewal capacity. The shared transcriptional programs and vulnerabilities between NCLSCs and cancer cells remains poorly understood. Here, we identify a developmental LPAR1-axis critical for NCLSC viability and melanoma cell survival. LPAR1 activity increased during progression and following acquisition of therapeutic resistance. Notably, genetic inhibition of LPAR1 potentiated BRAFi +/- MEKi efficacy and ablated melanoma migration and invasion. Our data defines LPAR1 as a new therapeutic target in melanoma and highlights the promise of dissecting stem cell-like pathways hijacked by tumor cells.

STATEMENT OF SIGNIFICANCE (50 words)

This study identifies an LPAR1-axis critical for melanoma invasion and intrinsic-/acquired-therapy resistance.

INTRODUCTION

Immense progress has been made for patients with advanced melanoma with 13 new FDA-approved therapies since 2011 (1, 2). The majority (76%) of patients whose melanomas harbor activating *BRAF*$^{V600E/K}$ mutations (~50% of patients) respond dramatically to dual BRAF/MEK inhibitor therapy (BRAFi/MEKi) (3). However, resistance arises within 2 years in near all cases, and four out of five of these patients show no long-term benefit with immunotherapy due to toxicity and/or non-responsiveness. This expanding BRAFi/MEKi-resistant patient cohort is the greatest challenge of the melanoma field as no alternative effective targeted therapies exist.

We and others have identified melanoma cells that dedifferentiate to a neural crest-like stem cell (NCLSC) state capable of surviving challenging environmental contexts including metastasis and therapy (4). Molecularly, these NCLSC-like melanoma cells express NCLSC markers including JARID1B (5), NGFR (6), EGFR (7), SerpinE2 (8) and/or AXL, as well as a NCLSC transcriptional signature (9). Biologically, NCLSC-like melanoma cells exhibit high invasiveness and plasticity. Critically, NCLSC-like melanoma cells are intrinsically resistant to chemo- and targeted therapy (4, 9). These findings underscore the need to develop novel therapeutic strategies that potently eliminate NCLSC-like melanoma cells and define the molecular mechanisms responsible for the therapy resistance and aggressive phenotypes of NCLSC-like melanoma cells.

Towards this goal, we executed a transcriptome juxtaposition study to compare gene expression profiles of human skin-derived NCLSCs, melanocytes and melanoma cultures. During embryonic development, multipotent trunk NCLSCs migrate from the neural plate to the epidermis/dermis and undergo lineage specification to generate differentiated melanocytes (10, 11). In turn, melanoma cells arise following the malignant transformation of melanocytes. We focused on genes highly expressed in both melanoma cells and NCLSCs, but not in melanocytes to identify genes associated with a dedifferentiated NCLSC state. This approach led to the delineation of a cluster of stem cell-like genes

enriched in melanoma. Using a targeted RNA interference strategy coupled with functional *in vitro* and *in vivo* studies, we have identified lysophosphatidic acid receptor 1 (LPAR1) as critical for targeted therapy-resistance in melanoma cells. LPAR1 is elevated in patient tumor tissue and drives melanoma proliferation, mobility, invasiveness and resistance to therapy by promoting mTOR and YAP activity. Our findings reveal an unanticipated role of LPAR1 in regulating both mTOR and YAP activity, and define LPAR1 as a novel target for the treatment of BRAFi/MEKi-resistant melanoma patients.

Materials and Methods

Additional molecular and cell biology techniques, list of oligonucleotides, high-throughput methods and detailed computational analyses are described in **Extended Experimental Procedures**.

Cell Culture of NCLSC, melanocytes and fibroblasts

NCLSC, melanocytes and fibroblasts were isolated from human foreskins and were cultured as previously described (12). Following the investigation of LPAR1 levels in a panel of 23 melanoma cell lines, 4 melanocyte cultures and 4 NCLSC cultures, we selected the top highest 3 LPAR1 expressing cell lines in the *BRAF*-MT cohort, with similar expression to that found in NCLSCs, as LPAR1 high. Conversely, we selected the lowest 3 LPAR1 expressing cell lines in the *BRAF*-MT cohort, with similar expression to melanocytes, as LPAR1 low cells. We also selected the top 3 highest LPAR1 expressing cell lines in the *NRAF*-MT cohort as LPAR1 high and the lowest 3 LPAR1 expressing cell lines in the *NRAS*-MT cohort as the LPAR1 low. All of the BRAF/NRAS-WT/WT cell lines had low LPAR1 expression akin to melanocytes.

Melanoma Patient scRNA-seq data

Invasive/NCSC/Nutrient depleted and Pigmented gene sets were derived from Rambow et al. Cell 2018 (9), and the Stress-like gene set was derived from Baron et al Cell Systems 2020 (13). Normalized single cell expression data from Tirosh et al Science 2016 paper (14) (GEO accession number GSE72056) was used to calculate cell expression signatures for 1257 tumor cells as an average

value among genes from the set. Expression signatures were compared using ttest between cells with no detected LPAR1 expression versus LPAR1 positive cells. Fold changes of mean LPAR1+/LPAR1- values were calculated.

Cell Lines Established from Human Melanomas and Patient-derived Xenografts

All normal skin epidermal melanocytes, keratinocytes, dermal stem cells and human metastatic melanoma cell lines that were established at The Wistar Institute have been documented (https://www.wistar.org/lab/meenhard-herlyn-dvm-dsc/page/resources). UACC-62 and UACC-903 cells were kind gifts from Dr. Marianne B. Powell (Stanford University, Stanford, CA 94305, USA). A375 cells were purchased from the ATCC. All resistant cell lines that acquired drug resistance to PLX4720 (hereafter referred to as “BR” cell lines) or the combination of PLX4720 and PD0325901 (hereafter referred to as “CR” cell lines) were established after continuous exposure to PLX4720 at 10 μM or the combination of PLX4720 at 10 μM and PD0325901 at 1 μM. All cell lines were maintained in Tumor media (MCDB and LC15) supplemented with 2% fetal bovine serum (FBS; Tissue Culture Biologicals) or DMEM media (Mediatech, Inc.) supplemented with 10% fetal bovine serum. Cells were cultured in a 37°C humidified incubator supplied with 5% CO_2. All cell lines were authenticated by DNA fingerprinting.

Accession Number

The GEO database accession number for the gene expression microarray and RNAseq data is GSE92765.

Drug Sensitivity IC50 Data

IC_{50} data for human melanoma cell lines with *BRAF*^{V600} mutations treated with selective BRAF and MEK inhibitors were curated from the Cancer Cell Line Encyclopedia (CCLE).

Reverse phase protein array (RPPA) and Analysis

The RPPA assay was performed by the MD Anderson Cancer Center RPPA core facility (Houston, TX) using the method described on the MD Anderson Cancer Center website. The same differential expression analysis method used for the microarray data was applied to RPPA data. Proteins that were most significantly down-regulated were clustered by their functional pathways and were used to generate the heatmaps.

Chemicals

The BRAF inhibitors PLX4032, PLX4720 and GSK2118436 and the MEK inhibitor PD0325901 were purchased from Selleckchem. For *in vivo* oral gavage, PLX4032 was suspended in Klucel EF 2% (w/v), and the pH was adjusted to 4 using HCl. The compound was dosed using feeding tubes (Instech Laboratories, Inc).

Cell Growth/Viability and Assessment of Cell Clonogenicity

Cell viability was measured by the MTT assay. For the assessment of cell clonogenicity, cells were seeded in 6-well tissue culture plates at a density of 4000 cells/well as biological triplicates in drug-free medium. Medium was refreshed every 2 or 3 days for 15-21 days. Colonies were then stained overnight with methanol containing 0.05% crystal violet. After extensive washing with distilled H_2O, cells were air-dried and subjected to image acquisition using an Epson scanner (Epson perfection V700 photo).

GST pull-down assay

The GST pull-down assay was carried out using an Active Rap1 Detection Kit (Cell Signaling) according to the manufacturer's instructions. Briefly, 50% glutathione resin slurry was bound to the column tube, followed by the addition of 20 µG GST-RalGDS-RBD. Cell lysates (1 mg total protein) from melanoma cells with different treatments were added to the column tube and incubated at 4°C for 1 hr. After 3 cycles of washing, the reducing sample buffer was added and the eluted samples were collected and subjected to SDS electrophoresis and Western blotting.

RESULTS

Transcriptome Juxtaposition and Targeted Screens Identify LPAR1

In an effort to identify shared stem cell-like programs between melanoma cells and neural crest-like stem cells (NCLSCs), gene expression profiles of human skin-derived NCLSC, melanocyte and melanoma cultures were juxtaposed to distinguish gene candidates enriched in NCLSC and melanoma cultures, but not melanocytes (**Figure 1A**). Analysis of gene expression microarray and RNA sequencing (RNA-Seq) data identified 98 (adjusted p-value<0.05, fold>2) and 122 (adjusted p-value<0.05) gene candidates, respectively, including novel and known (i.e., NGFR, PDGFRβ) drivers of melanoma aggressiveness (7, 15, 16) (**Figure 1A, Supplemental Table S1, Supplemental Figure 1A**), resulting in a set of 208 unique genes. To experimentally validate the functional relevance of these gene candidates on melanoma cell proliferation, a targeted RNA interference screen was executed (188 of the 208 genes were included in the siRNA library), which in addition included 52 genes that serve functional roles in stem cell biology, resulting in a set of 240 unique genes. Four distinct siRNA sequences were incorporated against each gene (8 genes IGFBP2, MEIS2, ODC1, PALLD, RASD1, TM4SF1, TNFRSF12A, TNFRSF21 were tested twice) along with the housekeeping gene EIF4A3 (K), 5 non-specific (NS) siRNA and a media only well (E). Two melanoma cell lines (one harboring a *BRAF*^{V600E} mutation, one harboring an *NRAS*^{Q61R} mutation) were included in the screen (**Figure 1B, Supplemental Table S2**). Approximately 19% of the gene candidates could inhibit melanoma cell proliferation by ≥ 25% across the melanoma cell lines. The top 31 gene candidates were subjected to a second independent validation screen (**Figure 1C, Supplemental Table S3**). Genes previously reported to contribute to melanoma aggressiveness and therapy resistance emerged both in our shared NCLSC and melanoma

transcriptome analysis and second validation screen, further supporting our hypothesis that novel therapeutic targets could be defined among genes associated with a dedifferentiated NCLSC state. Nerve growth factor receptor (NGFR) emerged in our screen, which is a canonical marker of de-differentiated melanoma cells that display adaptive resistance to BRAF inhibition (6), and melanoma cells resistant to anti-PD-1 blockade (17). The Notch signaling ligand, delta like canonical notch ligand 4 (DLL4), emerged in our screen, which agrees with the literature showing a role for notch signaling in promoting cancer stem cell viability through tissue remodeling (18). Connective tissue growth factor (CTGF) was detected in our screen and has been reported to increase in AML-derived mesenchymal stem cells (19) and serve a critical role in the metastatic capacity of melanoma cells (20). Ribonucleotide reductase regulatory subunit M2 (RRM2), Baculoviral IAP repeat containing 5 (BIRC5) and KDEL endoplasmic reticulum protein retention receptor 3 (KDELR3) are additional genes that were detected in our screen that have been previously shown to play a role in melanoma metastasis and therapy resistance (21-23). The top gene candidates were next evaluated by Ingenuity Pathway Analysis software, which identified a lysophosphatidic acid receptor 1 (LPAR1)-axis as a critical signaling network (**Figure 1D, Supplemental Figure 1B**). LPAR1 is a G12/13-coupled receptor that drives the proliferation of neuronal progenitor cells (24), and promotes the aggressiveness of breast (25), lung (26), and ovarian cancer (27). Interrogation of LPAR1 expression in an extended panel of NCLSC, melanocyte and melanoma cultures confirmed melanoma cells exhibit higher expression levels of LPAR1 relative to melanocytes (**Figure 1E**). A subset of 5 *BRAF*-mutant and 3 *NRAS*-mutant melanoma cell lines display higher levels of LPAR1 relative to melanocytes and equivalent to those in NCLSCs (**Figure 1E**). Conversely, a subset of 4 *BRAF*-mutant and 3 *NRAS*-mutant melanoma cell lines display relatively low LPAR1 expression levels akin to those observed in melanocytes. LPAR1 expression within *BRAF/NRAS*-wildtype/wildtype melanoma cells is lower overall relative to other genotypes (**Figure 1E**). Collectively, these data identify LPAR1 as a stem cell gene enriched in subsets of *BRAF*-MT and *NRAS*-MT melanoma cells.

LPAR1 Sustains Melanoma and NCLSC Survival

A subset of 3 *BRAF*-mutant and 3 *NRAS*-mutant melanoma cell lines with the highest levels of LPAR1 (hereafter called LPAR1^{hi} cells) and a subset of 3 *BRAF*-mutant and 3 *NRAS*-mutant melanoma cell lines with the lowest levels of LPAR1 (hereafter called LPAR1^{lo} cells) were chosen to perform additional analyses to understand the functional role of LPAR1 in melanoma. We found that ectopic addition of lysophosphatidic acid (LPA), the activating ligand of LPAR1, increases the proliferation of a subset of melanoma cell lines across different genotypes (**Figure 2A, Supplemental Figure 2A**), which was positively correlated to LPAR1 expression (**Figure 1E**) (28). Notably, LPAR1 expression correlated with sensitivity to genetic silencing of LPAR1, whereby *BRAF*-mutant melanoma cell lines with high LPAR1 expression (LPAR1^{hi}) display significant inhibition of proliferation following siLPAR1 (**Figure 2B, Supplemental Figure 2B**). In contrast, *BRAF*-mutant melanoma cells or normal cells (i.e., melanocytes, fibroblasts) with low LPAR1 expression (LPAR1^{lo}) experience reduced or no cytotoxicity, with the exception of the WM46 cell line. Loss of LPAR1 with shRNA also blunted the long-term colony forming capacity of LPAR1^{hi} melanoma cells, in contrast to LPAR1^{lo} melanoma cells (**Figure 2C, Supplemental Figure 2D**). The positive relationship between LPAR1 expression and genetic silencing of LPAR1-induced inhibition of proliferation was also observed in *NRAS*-mutant melanoma cells (**Supplemental Figure 2C**). In accordance, genetic silencing of LPAR1 induces NCLSC cytotoxicity (**Supplemental Figure 2E**). Collectively, these data demonstrate the importance of LPAR1 for NCLSCs and LPAR1^{hi} melanoma cells independent of genotype.

LPAR1 Drives Melanoma Migration and Invasion.

We next interrogated the role of LPAR1 in melanoma invasiveness. LPAR1 has been reported to promote metastasis of breast and ovarian cancer (29, 30). In wound healing and transwell migration assays, genetic inhibition of LPAR1 reduced wound closure and migratory capacity of LPAR1^{hi} melanoma cells grown in complete media, respectively (**Figure 3A, 3B**). In Boyden chamber assays, genetic (shLPAR1) inhibition of LPAR1 also reduced melanoma invasiveness (**Figure 3C**). To better recapitulate the normal physiology of the skin, we established human skin reconstructs including LPAR1^{hi} melanoma cells transfected with siLPAR1, which decreased melanoma proliferation and invasion (**Figure**

3D, Supplemental Figure 3B) (31). To ensure our observations on melanoma invasion were independent of the impact of LPAR1 inhibition on melanoma viability, we performed extracellular matrix degradation assays demonstrating viable melanoma cells expressing shLPAR1 have reduced ability to degrade gelatin (**Supplemental Figure 3A**). Taken together, these results suggest that LPAR1 signaling plays an important role in promoting melanoma migration and invasion.

LPA Regulates LPAR1 Signaling through a RAPGEF5-RAP1A-Axis

We next dissected the requisite molecules for LPAR1 signal transduction using *BRAF*-MT melanoma cells. RAP-GTPases have been reported to be regulated by LPAR receptors (32, 33). Two members of the RAS subfamily of GTPases (RAP1A and RAPGEF5) emerged from our targeted siRNA screen (**Figure 1**). In accordance, overexpression of RAPGEF5 could rescue proliferation in melanoma cells expressing shLPAR1 (**Figure 4A, Supplemental Figure 4A**). Further, expression of a constitutively active RAP1A (Q63E) mutant rescues proliferation in shLPAR1 melanoma cells, whereas expression of the constitutively inactive RAP1A (S17N) mutant does not rescue proliferation. To more directly examine the role of LPAR1 on RAP1A activity, a GST pull-down assay was performed using GST-tagged RAP binding domain (RBD) of RalGDS (GST-RalGDS-RBD), a direct downstream effector of RAP1A that specifically binds to active RAP1A (34). RAP1A activity is suppressed in shLPAR1 melanoma cells, as evidenced by a decrease in GST-RalGDS-GBD levels in pulldown lysate (**Figure 4B**). Activation of LPAR1 following ectopic LPA hyperactivates RAP1A, which is ablated by genetic silencing of RAPGEF5 (**Figure 4C**). In concordance, overexpression of RAPGEF5 recovers RAP1A activity in shLPAR1 melanoma cells (**Figure 4D**). Although acute genetic silencing of RAPGEF5 did not cause significant inhibition of cell growth (Figure 1C), long-term genetic silencing of RAPGEF5 and RAP1A reduces colony formation only in LPAR1^{hi} melanoma cells (**Figure 4E, Supplemental Figure 4B**). Genetic silencing of RAPGEF5 and RAP1A also ablates melanoma invasiveness (**Figure 4F**) and decreases proliferation in human skin reconstructs (**Figure 4G, Supplemental Figure 4C, 4D, 4E, 4F**). As LPAR1 is a G12/13-coupled receptor (35), we confirmed the importance of G12/13 in the transduction of LPAR1 survival

signals in LPAR1^{hi} melanoma cells (**Supplemental Figure 4G, 4H, 4I**). Indeed, silencing of G12/13 phenocopies the effect of genetic silencing of LPAR1 on proliferation. Proliferation could not be rescued following siG12/13 by ectopic LPA treatment demonstrating its role downstream of LPAR1. Collectively, these data demonstrate LPAR1 signal transduction locally transmits through a RAPGEF5-RAP1A-axis.

mTOR and YAP are Downstream Effectors of LPAR1-Axis

LPAR1 stimulation by LPA has been previously shown to induce downstream YAP1 activation (35) and activation of the PI3K-mTOR pathway (36). To gain further mechanistic insight into LPAR1 signal transduction in melanoma, we exploited a systems biology approach to investigate functional proteomic alterations following LPAR1 inhibition. In agreement, reverse phase protein arrays (RPPA) revealed a signature associated with inactivation of YAP (TAZ), as well as inhibition of mTOR (pS6, p4E-BP1) and cell cycle progression (cyclin B1, pRb) following LPAR1 inhibition (**Figure 5A, Supplemental Table S4**). Notably, genetic (siLPAR1) inhibition of LPAR1 inactivates mTOR and inhibits YAP/TAZ as validated by Western blotting specifically in LPAR1^{hi} melanoma cells across genotypes (**Figure 5B, Supplemental Figure 5A**). Phosphorylation of YAP at S127 inactivates YAP by promoting its translocation from the nucleus to the cytoplasm (37). Genetic silencing of LPAR1 triggers cytoplasmic expression of YAP (**Figure 5C**). Notably, genetic silencing of neither YAP or S6K could achieve equivalent suppression of long-term clonogenic growth to silencing of LPAR1 (**Figure 5D**). However concurrent silencing of S6K and YAP more completely blunted clonogenic growth only in LPAR1^{hi} melanoma cells suggesting LPAR1 promotes melanoma cell cycle progression via both mTOR and YAP signaling (**Supplemental Figure 5B, 5C**).

LPAR1 Promotes Intrinsic and Acquired Resistance to Targeted Therapy

We next interrogated the role LPAR1 serves in the context of targeted therapy. Publicly available genome-wide expression data in the TCGA revealed LPAR1^{hi} melanoma cells express a negative

correlation with a master lineage regulator in melanocytes, MITF, and a positive correlation with a de-differentiated melanoma marker, AXL (**Figure 6A**). To place LPAR1^{hi} cells into context with other recently characterized therapy resistant melanoma subpopulations (i.e., NCSC, invasive, pigmented, stress-like cancer cell) (9, 13, 38), we analyzed publicly available scRNAseq datasets that revealed LPAR1^{hi} cells significantly correlate with a recently reported neural crest stem cell melanoma subpopulation that plays a role during minimal residual disease (**Supplemental Figure 6A**) (9, 14). In agreement, LPAR1^{hi} cells possess intrinsic resistance to MAPK pathway inhibitors (MAPKi) (39) (**Supplemental Figure 6B, 6C, 6D**). LPAR1^{hi} melanoma cell lines are less sensitive to BRAF inhibitor (PLX4720) and MEK inhibitor (PD0325901, AZD6244) therapy relative to LPAR1^{lo} melanoma cells. No difference in β-catenin levels are observable between LPAR1^{hi} and LPAR1^{lo} cells (**Supplemental Figure 6E**). Notably, LPAR1 expression increases in LPAR1^{lo} melanoma cell lines (**Figure 6B**) and patient-derived xenograft models (**Supplemental Figure 6F**) once resistance to BRAFi or BRAFi/MEKi is acquired. LPAR1 is functional in acquired therapy resistance, as genetic (siLPAR1) targeting of LPAR1 impairs proliferation (**Figure 6C, Supplemental Figure 6G**) and blunts long-term colony formation **Supplemental Figure 6H**) exclusively in melanoma cells with acquired BRAFi- or BRAFi/MEKi-resistance, whereas paired parental cells displayed little to no sensitivity. Further, genetic silencing of RAGPEF or RAP1A phenocopied these effects in therapy resistant melanoma cells (**Supplemental Figure 6H**). Genetic silencing of LPAR1 also increased the efficacy of BRAFi (**Supplemental Figure 6I**). RPPA analyses revealed that melanoma cells with acquired BRAFi/MEKi-resistance display higher phosphorylation of Rb at S807 (associated with elevated cell cycle progression) and higher mTOR activity (increased phosphorylation of S6 and 4E-BP1) relative to therapy naïve parental cells, which has been reported to denote therapy refractory melanomas (40) (**Figure 6D, Supplemental Table S5**). Genetic silencing of LPAR1 significantly inhibited cell cycle progression (decreased cyclin B1 and pRb S807), decreased mTOR activity (decreased pS6 and p4E-BP1) and blunted YAP activity (increased pYAP S127), which was validated by Western blotting (**Figure 6D, 6E**). Notably, genetic (siLPAR1) inhibition of LPAR1 does not inhibit the MAPK pathway in melanoma cells. Taken together, these data

reveal LPAR1 promotes intrinsic and acquired resistance to BRAFi and BRAFi/MEKi by sustaining mTOR and YAP activity.

We next investigated the *in vivo* relevance of LPAR1 in tumorigenesis. Staining of a large set patient tissue derived from benign nevi, primary melanoma and melanoma metastases revealed a striking increase in LPAR1 expression in primary and metastatic melanoma tumor tissue from patients versus benign nevi (**Figure 6F**). To characterize the *in vivo* antitumor activity of targeting LPAR1, melanoma xenografts were established in the flanks of NSG mice using the WM9 cell line expressing shLuc or shLPAR1 (**Figure 6G, Supplemental Figure 6J**). Genetic inhibition of LPAR1 had a significant effect on tumor growth, mTOR signaling and YAP activity relative to control tumors (**Supplemental Figure 6K**). Notably, the anti-tumor BRAFi efficacy is significantly increased in tumor cells expressing shLPAR1 relative to control tumors (**Figure 6G**). Altogether, these data suggest the stem cell-like LPAR1-axis is reduced in NCSLCs as they differentiate into melanocytes and increased in a subset of melanoma cultures that possess intrinsic resistance to therapy (**Figure 6H**). Notably, LPAR1 expression is elevated in therapy-naïve cells following the acquisition of resistance to BRAFi and/or MEKi, representing a novel target to increase therapy efficacy.

DISCUSSION

Tumor cells often hijack stem cell-like pathways active in their normal progenitor cells favoring tumor growth and survival (41, 42). Identifying and dissecting the stem cell-like pathways that are responsible for the maintenance of normal stem cells thus has the potential to help us better define tumor-specific changes and to discover novel therapeutic approaches. There are an increasing number of studies that show correlations between genes that regulate neural crest/melanocyte development and their contribution to melanoma tumorigenesis (4, 7-9, 43, 44). By integrating combinatorial gene knockout approaches, cell-based assays and immune-histochemical observations, recent studies have illustrated several genes and pathways including Wnt (45) and Sox (46) proteins that serve important roles in melanocyte specification and melanoma progression (47). The evidence that high WNT5A expression also correlates with a $MITF^{lo}/AXL^{hi}$ signature and that YAP signaling serves as a downstream effector of

WNT5A would suggest that LPAR1 and WNT5A may co-regulate downstream YAP signaling through distinct yet parallel pathways (48). Further, YAP has been shown to rescue *RAS*-mutant cancer cell viability following suppression of *KRAS* in *KRAS*-mutant colon cancer cells (49) and MEK inhibition in *NRAS*-mutant melanoma cells (50), with evidence that KRAS and YAP converge to regulate epithelial mesenchymal transition (EMT) and tumor survival.

Using zebrafish, a chemical screen recently identified small-molecule suppressors of the neural crest lineage that may have inhibitory effects on melanoma (51). However, a systematic investigation of human cells is still lacking to directly explore shared gene signatures between NCLSCs and melanoma cells for translational studies. In this study, we took advantage of our extensive collection of melanoma cell lines and normal human skin-derived melanocytes to compare them with human skin-derived NCLSCs that behave similarly to embryonic neural crest cells (12). Using a systems biology approach in which computational analyses were coupled with targeted siRNA screens, we identified a panel of genes up-regulated both in NCLSC and melanoma cells, but not in melanocytes. To our knowledge, this is the first study where the common gene signature shared between NCLSCs and melanoma cells was subjected to computational prediction, biological assays and functional characterization.

We here identify that LPAR1 is upregulated in NCLSC and melanoma cells relative to melanocytes. LPAR1 is highly expressed in regions of the central nervous system during embryonic neurogenesis and serves a role in stem cell processes (52). LPA signaling functions in nervous system processes, such as the mobilization of intracellular calcium, changes in neuroblast and neuron conductance, and survival and migration of Schwann cells (53). LPA gradients have previously been shown to be a major driver of melanoma chemotaxis (54, 55). To our knowledge, no previous connection between LPA or LPAR1 and targeted therapy (i.e., BRAFi/MEKi resistance) has been made in the melanoma field. In this study, we observe inhibition of LPAR1 signaling disrupts the acquisition of resistance. Further, LPAR1 drives the formation of stem cell spheres. Collectively, these data suggest that LPA signaling plays a vital role in cells with stem cell-like properties.

RAP small GTPases are one group of downstream effectors of LPA signaling that can be activated via G proteins or specific GDP/GTP exchange factors (GEFs) (56). We identified RAPGEF5

and RAP1A as critical for the local signal transduction of LPAR1. Through functional rescue experiments and GST pull-down assays, we discovered that RAP1A is a direct downstream effector of LPAR1 signaling that is regulated through RAPGEF5 by LPAR1. Collectively, these results underscore a core-signaling network comprised of LPAR1, RAPGEF5 and RAP1A in melanoma. LPAR1 is a widely expressed LPAR receptor that is up-regulated in advanced cancers including ovarian and breast cancer, and has been implicated in promoting aggressiveness and metastasis in these tumors (29, 57). Our work investigates the functions of LPAR1 in melanoma and demonstrates that LPAR1-RAPGEF5-RAP1A signaling is required for the growth, viability and invasiveness of LPAR1^{hi} melanoma cells, independent of genotype.

LPA signaling has been previously reported to regulate cell survival signaling through two main pathways; the PI3K/AKT (58) and the RAS/MAPK pathways (59). Interestingly, we did not observe any significant alterations of pERK or pAKT levels upon genetic inhibition of LPAR1 signaling. These findings indicate that LPAR1 signaling does not contribute to human melanoma cell growth through the canonical MAPK or PI3K/AKT pathways, but rather via alternative downstream effectors. Strikingly, we find LPAR1 inhibition results in the potent and concurrent inactivation of YAP and mTOR signaling in melanoma, in agreement with previous reports (35). LPA can stimulate the nuclear accumulation of YAP, resulting in YAP activation (35), however its role in mTOR is novel in melanoma. mTOR (60) and YAP (61) have both been implicated as resistance mechanisms against MAPK inhibitors in melanoma. YAP downregulation has been shown to sensitize BRAFi-resistant melanoma cells to MAPK pathway inhibitors, and YAP and Wnt signaling (via β-catenin-LEF1) co-regulate apoptosis of acquired MAPK inhibitor-resistant melanoma (62). LPAR1 inhibition inhibits melanoma growth by loss of both mTOR and YAP activity as shown by cells expressing either shS6K or shYAP not able to achieve the equivalent level of growth suppression relative to shLPAR1. Concurrently silencing both S6K and YAP could achieve equivalent growth suppression to shLPAR1, notably only in LPAR1^{hi} melanoma cells. These data suggest LPAR1 expression could serve as a biomarker for melanoma cells that heavily rely on mTOR and YAP activity.

Collectively, our studies establish the molecular basis of how the LPAR1-RAPGEF5-RAP1A

signaling axis underlies both intrinsic- and acquired- drug resistance to targeted therapies for *BRAF*$^{V600E/K}$ melanoma cells. We also provide a rationale for combining inhibitors of LPAR1 signaling with FDA approved MAPK inhibitors to trigger synthetic lethality both in innate resistant and in acquired resistant cells. Our data warrant further investigation of prognostic biomarkers of LPAR1 signaling that could predict success in combining LPAR1 inhibitors and targeted therapies to overcome both intrinsic- and acquired-therapy resistance by expanding *in vitro* and *in vivo* models. To date, there have been a number of melanoma subpopulations characterized to drive therapy resistance including NCSC-like (6), invasive (9), pigmented and a recently identified stress subpopulation that all exhibit transient yet detectable levels of differentiation/dedifferentiation (13). We believe our LPAR1 studies yield an actionable vulnerability necessary for dedifferentiated NCSC-like melanoma cells to persist and drive therapy resistance. In summary, these data provide the scientific rationale to clinically explore LPAR1 as a novel therapeutic target for therapy-naïve patients as well as in patients with melanomas that are intrinsically resistant or have developed acquired resistant to targeted therapies. As LPAR1 is important for the maintenance and growth of stem cells, it will be interesting to further examine the link between LPAR1 signaling and melanoma stem-like cells. Future studies of the functions of LPAR1 signaling in other types of cancers and its potential role in response to immunotherapy are needed.

Author Contributions

JL, VWR and MH designed the study. JL, TC, AG, CCY, CT, YH, CK, MD, LL, MX, ASM, KS, JW, MB, AV, DH, LWW, YL, GZ, AS, DZ, JZ, CC, GA, MFK, BD, YH, PB, DWS and VWR conducted experiments. JL, VWR, TC, JZ, CC, PAB, CT, KS, PAB, LWW, ZW, AVK, QL analyzed data. WX, GCK, XX, LMS, TCM, RKA, LNK, DTF, GMB and KTF provided patients' samples, clinical information and expression array data. JL, VWR, and MH wrote the paper, with input and scientific advice from MFK, GZ, ZR, GBM, RS, ZW, TC, WX, JSM and AG.

Acknowledgements

We thank all former and current lab members for comments and helpful discussions; J. Hayden and F. Keeney (Wistar Microscopy Facility), C. Chang, S. Billouin, and T. Nguyen (Wistar Genomics Facility), and J.S. Faust and D. Ambrose (Wistar Flow Cytometry Facility) for technical support. We apologize to those whose work was not cited or mentioned here due to space constraints. The research was funded by NIH grants P01 CA114046, P01 CA025874, P30 CA010815, R01 CA047159, K01CA245124 and by the Dr. Miriam and Sheldon G. Adelson Medical Research Foundation and the Melanoma Research Foundation. The support for Shared Resources utilized in this study was provided by Cancer Center Support Grant (CCSG) CA010815 and S10 OD023586 to the Wistar Institute.

REFERENCES

1. Carlino MS, Long GV, Schadendorf D, Robert C, Ribas A, Richtig E, et al. Outcomes by line of therapy and programmed death ligand 1 expression in patients with advanced melanoma treated with pembrolizumab or ipilimumab in KEYNOTE-006: A randomised clinical trial. Eur J Cancer. 2018;101:236-43. Epub 2018/08/11. doi: 10.1016/j.ejca.2018.06.034. PubMed PMID: 30096704.
2. Dummer R, Ascierto PA, Gogas HJ, Arance A, Mandala M, Liszkay G, et al. Overall survival in patients with BRAF-mutant melanoma receiving encorafenib plus binimetinib versus vemurafenib or encorafenib (COLUMBUS): a multicentre, open-label, randomised, phase 3 trial. Lancet Oncol. 2018;19(10):1315-27. Epub 2018/09/17. doi: 10.1016/s1470-2045(18)30497-2. PubMed PMID: 30219628.
3. Long GV, Eroglu Z, Infante J, Patel S, Daud A, Johnson DB, et al. Long-Term Outcomes in Patients With BRAF V600-Mutant Metastatic Melanoma Who Received Dabrafenib Combined With Trametinib. J Clin Oncol. 2018;36(7):667-73. Epub 2017/10/11. doi: 10.1200/jco.2017.74.1025. PubMed PMID: 28991513.

4. Roesch A, Vultur A, Bogeski I, Wang H, Zimmermann KM, Speicher D, et al. Overcoming intrinsic multidrug resistance in melanoma by blocking the mitochondrial respiratory chain of slow-cycling JARID1B(high) cells. Cancer Cell. 2013;23(6):811-25. Epub 2013/06/15. doi: 10.1016/j.ccr.2013.05.003. PubMed PMID: 23764003; PMCID: PMC3810180.
5. Roesch A, Fukunaga-Kalabis M, Schmidt EC, Zabierowski SE, Brafford PA, Vultur A, et al. A temporarily distinct subpopulation of slow-cycling melanoma cells is required for continuous tumor growth. Cell. 2010;141(4):583-94. Epub 2010/05/19. doi: 10.1016/j.cell.2010.04.020. PubMed PMID: 20478252; PMCID: PMC2882693.
6. Fallahi-Sichani M, Becker V, Izar B, Baker GJ, Lin JR, Boswell SA, et al. Adaptive resistance of melanoma cells to RAF inhibition via reversible induction of a slowly dividing de-differentiated state. Mol Syst Biol. 2017;13(1):905. Epub 2017/01/11. doi: 10.15252/msb.20166796. PubMed PMID: 28069687; PMCID: PMC5248573.
7. Shaffer SM, Dunagin MC, Torborg SR, Torre EA, Emert B, Krepler C, et al. Rare cell variability and drug-induced reprogramming as a mode of cancer drug resistance. Nature. 2017;546(7658):431-5. Epub 2017/06/14. doi: 10.1038/nature22794. PubMed PMID: 28607484; PMCID: PMC5542814.
8. Perego M, Maurer M, Wang JX, Shaffer S, Muller AC, Parapatics K, et al. A slow-cycling subpopulation of melanoma cells with highly invasive properties. Oncogene. 2018;37(3):302-12. Epub 2017/09/20. doi: 10.1038/onc.2017.341. PubMed PMID: 28925403; PMCID: PMC5799768.
9. Rambow F, Rogiers A, Marin-Bejar O, Aibar S, Femel J, Dewaele M, et al. Toward Minimal Residual Disease-Directed Therapy in Melanoma. Cell. 2018;174(4):843-55.e19. Epub 2018/07/19. doi: 10.1016/j.cell.2018.06.025. PubMed PMID: 30017245.
10. Dupin E, Calloni G, Real C, Goncalves-Trentin A, Le Douarin NM. Neural crest progenitors and stem cells. C R Biol. 2007;330(6-7):521-9. Epub 2007/07/17. doi: 10.1016/j.crvi.2007.04.004. PubMed PMID: 17631447.
11. Cichorek M, Wachulska M, Stasiewicz A, Tyminska A. Skin melanocytes: biology and development. Postepy Dermatol Alergol. 2013;30(1):30-41. Epub 2013/11/28. doi: 10.5114/pdia.2013.33376. PubMed PMID: 24278043; PMCID: PMC3834696.
12. Li L, Fukunaga-Kalabis M, Yu H, Xu X, Kong J, Lee JT, et al. Human dermal stem cells differentiate into functional epidermal melanocytes. J Cell Sci. 2010;123(Pt 6):853-60. Epub 2010/02/18. doi: 10.1242/jcs.061598. PubMed PMID: 20159965; PMCID: PMC2831759.
13. Baron M, Tagore M, Hunter MV, Kim IS, Moncada R, Yan Y, et al. The Stress-Like Cancer Cell State Is a Consistent Component of Tumorigenesis. Cell Syst. 2020;11(5):536-46.e7. Epub 2020/09/11. doi: 10.1016/j.cels.2020.08.018. PubMed PMID: 32910905.
14. Tirosh I, Izar B, Prakadan SM, Wadsworth MH, 2nd, Treacy D, Trombetta JJ, et al. Dissecting the multicellular ecosystem of metastatic melanoma by single-cell RNA-seq. Science. 2016;352(6282):189-96. Epub 2016/04/29. doi: 10.1126/science.aad0501. PubMed PMID: 27124452; PMCID: PMC4944528.
15. Nazarian R, Shi H, Wang Q, Kong X, Koya RC, Lee H, et al. Melanomas acquire resistance to B-RAF(V600E) inhibition by RTK or N-RAS upregulation. Nature. 2010;468(7326):973-7. Epub 2010/11/26. doi: 10.1038/nature09626. PubMed PMID: 21107323; PMCID: PMC3143360.
16. Alonso-Curbelo D, Riveiro-Falkenbach E, Perez-Guijarro E, Cifdaloz M, Karras P, Osterloh L, et al. RAB7 controls melanoma progression by exploiting a lineage-specific wiring of the endolysosomal pathway. Cancer Cell. 2014;26(1):61-76. Epub 2014/07/02. doi: 10.1016/j.ccr.2014.04.030. PubMed PMID: 24981740.
17. Boshuizen J, Vredevoogd DW, Krijgsman O, Ligtenberg MA, Blankenstein S, de Bruijn B, et al. Reversal of pre-existing NGFR-driven tumor and immune therapy resistance. Nat Commun. 2020;11(1):3946. Epub 2020/08/10. doi: 10.1038/s41467-020-17739-8. PubMed PMID: 32770055; PMCID: PMC7414147 research support from Novartis, BMS, and NanoString, and has

received honoraria or consultation fees for MSD, BMS, Roche, Novartis, GSK, Pfizer, Lilly, Genmab, and Pierre Fabre. C.U.B. and D.S.P. are co-founders, shareholders and advisors of Immagene B.V. M.A.L. is co-founder, shareholder and CEO of Immagene B.V., unrelated to this study. K.T.F. has served on the Board of Directors of Clovis Oncology, Strata Oncology, Loxo Oncology, and Checkmate Pharmaceuticals; Scientific Advisory Boards of X4 Pharmaceuticals, PIC Therapeutics, Sanofi, Amgen, Asana, Adaptimmune, Fount, Aeglea, Shattuck Labs, Tolero, Apricity, Oncoceutics, Fog Pharma, Neon, Tvardi, xCures, Monopteros, and Vibliome; consultant to Lilly, Novartis, Genentech, BMS, Merck, Takeda, Verastem, Boston Biomedical, Pierre Fabre, and Debiopharm; and research funding from Novartis and Sanofi. G.M.B. has sponsored research agreements with Olink Pharmaceuticals, Palleon Pharmaceuticals, and Takeda Oncology. She has been on scientific advisory boards for Nectar Therapeutics and Novartis and served as a speaker for Novartis. All the other authors declare no competing interests.

18. Venkatesh V, Nataraj R, Thangaraj GS, Karthikeyan M, Gnanasekaran A, Kaginelli SB, et al. Targeting Notch signalling pathway of cancer stem cells. Stem Cell Investig. 2018;5:5-. doi: 10.21037/sci.2018.02.02. PubMed PMID: 29682512.

19. Li H, Li J, Cheng J, Chen X, Zhou L, Li Z. AML-derived mesenchymal stem cells upregulate CTGF expression through the BMP pathway and induce K562-ADM fusiform transformation and chemoresistance. Oncol Rep. 2019;42(3):1035-46. Epub 2019/07/20. doi: 10.3892/or.2019.7237. PubMed PMID: 31322275; PMCID: PMC6667869.

20. Finger EC, Cheng CF, Williams TR, Rankin EB, Bedogni B, Tachiki L, et al. CTGF is a therapeutic target for metastatic melanoma. Oncogene. 2014;33(9):1093-100. Epub 2013/02/26. doi: 10.1038/onc.2013.47. PubMed PMID: 23435419; PMCID: PMC3965577.

21. Aird KM, Zhang G, Li H, Tu Z, Bitler BG, Garipov A, et al. Suppression of nucleotide metabolism underlies the establishment and maintenance of oncogene-induced senescence. Cell reports. 2013;3(4):1252-65. Epub 2013/04/09. doi: 10.1016/j.celrep.2013.03.004. PubMed PMID: 23562156; PMCID: PMC3840499.

22. McKenzie JA, Liu T, Jung JY, Jones BB, Ekiz HA, Welm AL, et al. Survivin promotion of melanoma metastasis requires upregulation of alpha5 integrin. Carcinogenesis. 2013;34(9):2137-44. Epub 2013/05/04. doi: 10.1093/carcin/bgt155. PubMed PMID: 23640047; PMCID: PMC3765044.

23. Marie KL, Sassano A, Yang HH, Michalowski AM, Michael HT, Guo T, et al. Melanoblast transcriptome analysis reveals pathways promoting melanoma metastasis. Nature communications. 2020;11(1):333. Epub 2020/01/18. doi: 10.1038/s41467-019-14085-2. PubMed PMID: 31949145; PMCID: PMC6965108.

24. Park H, Kim S, Rhee J, Kim HJ, Han JS, Nah SY, et al. Synaptic enhancement induced by gintonin via lysophosphatidic acid receptor activation in central synapses. J Neurophysiol. 2015;113(5):1493-500. Epub 2014/12/17. doi: 10.1152/jn.00667.2014. PubMed PMID: 25505112.

25. Marshall JC, Collins JW, Nakayama J, Horak CE, Liewehr DJ, Steinberg SM, et al. Effect of inhibition of the lysophosphatidic acid receptor 1 on metastasis and metastatic dormancy in breast cancer. J Natl Cancer Inst. 2012;104(17):1306-19. Epub 2012/08/23. doi: 10.1093/jnci/djs319. PubMed PMID: 22911670; PMCID: PMC3611817.

26. Magkrioti C, Oikonomou N, Kaffe E, Mouratis MA, Xylourgidis N, Barbayianni I, et al. The Autotaxin-Lysophosphatidic Acid Axis Promotes Lung Carcinogenesis. Cancer Res. 2018;78(13):3634-44. Epub 2018/05/05. doi: 10.1158/0008-5472.Can-17-3797. PubMed PMID: 29724718.

27. Zhang G, Cheng Y, Zhang Q, Li X, Zhou J, Wang J, et al. ATXLPA axis facilitates estrogeninduced endometrial cancer cell proliferation via MAPK/ERK signaling pathway. Mol Med Rep. 2018;17(3):4245-52. Epub 2018/01/13. doi: 10.3892/mmr.2018.8392. PubMed PMID: 29328374; PMCID: PMC5802196.

28. Lin ME, Herr DR, Chun J. Lysophosphatidic acid (LPA) receptors: signaling properties and disease relevance. Prostaglandins Other Lipid Mediat. 2010;91(3-4):130-8. Epub 2010/03/25. doi: 10.1016/j.prostaglandins.2009.02.002. PubMed PMID: 20331961; PMCID: PMC2845529.
29. Sahay D, Leblanc R, Grunewald TG, Ambatipudi S, Ribeiro J, Clezardin P, et al. The LPA1/ZEB1/miR-21-activation pathway regulates metastasis in basal breast cancer. Oncotarget. 2015;6(24):20604-20. Epub 2015/06/23. doi: 10.18632/oncotarget.3774. PubMed PMID: 26098771; PMCID: PMC4653029.
30. Seo EJ, Kwon YW, Jang IH, Kim DK, Lee SI, Choi EJ, et al. Autotaxin Regulates Maintenance of Ovarian Cancer Stem Cells through Lysophosphatidic Acid-Mediated Autocrine Mechanism. Stem Cells. 2016;34(3):551-64. Epub 2016/01/23. doi: 10.1002/stem.2279. PubMed PMID: 26800320.
31. Li L, Fukunaga-Kalabis M, Herlyn M. The three-dimensional human skin reconstruct model: a tool to study normal skin and melanoma progression. J Vis Exp. 2011(54). Epub 2011/08/19. doi: 10.3791/2937. PubMed PMID: 21847077; PMCID: PMC3155964.
32. Kelley GG, Reks SE, Smrcka AV. Hormonal regulation of phospholipase Cepsilon through distinct and overlapping pathways involving G12 and Ras family G-proteins. Biochem J. 2004;378(Pt 1):129-39. Epub 2003/10/22. doi: 10.1042/bj20031370. PubMed PMID: 14567755; PMCID: PMC1223921.
33. Li Y, Kim JG, Kim HJ, Moon MY, Lee JY, Kim J, et al. Small GTPases Rap1 and RhoA regulate superoxide formation by Rac1 GTPases activation during the phagocytosis of IgG-opsonized zymosans in macrophages. Free Radic Biol Med. 2012;52(9):1796-805. Epub 2012/02/15. doi: 10.1016/j.freeradbiomed.2012.02.004. PubMed PMID: 22330068.
34. Albright CF, Giddings BW, Liu J, Vito M, Weinberg RA. Characterization of a guanine nucleotide dissociation stimulator for a ras-related GTPase. Embo j. 1993;12(1):339-47. Epub 1993/01/01. PubMed PMID: 8094051; PMCID: PMC413211.
35. Yu FX, Zhao B, Panupinthu N, Jewell JL, Lian I, Wang LH, et al. Regulation of the Hippo-YAP pathway by G-protein-coupled receptor signaling. Cell. 2012;150(4):780-91. Epub 2012/08/07. doi: 10.1016/j.cell.2012.06.037. PubMed PMID: 22863277; PMCID: PMC3433174.
36. Cui R, Cao G, Bai H, Zhang Z. LPAR1 regulates the development of intratumoral heterogeneity in ovarian serous cystadenocarcinoma by activating the PI3K/AKT signaling pathway. Cancer Cell International. 2019;19(1):201. doi: 10.1186/s12935-019-0920-0.
37. Lee Y, Kim NH, Cho ES, Yang JH, Cha YH, Kang HE, et al. Dishevelled has a YAP nuclear export function in a tumor suppressor context-dependent manner. Nature communications. 2018;9(1):2301. Epub 2018/06/14. doi: 10.1038/s41467-018-04757-w. PubMed PMID: 29895829; PMCID: PMC5997650.
38. Verfaillie A, Imrichova H, Atak ZK, Dewaele M, Rambow F, Hulselmans G, et al. Decoding the regulatory landscape of melanoma reveals TEADS as regulators of the invasive cell state. Nat Commun. 2015;6:6683. Epub 2015/04/14. doi: 10.1038/ncomms7683. PubMed PMID: 25865119; PMCID: PMC4403341.
39. Barretina J, Caponigro G, Stransky N, Venkatesan K, Margolin AA, Kim S, et al. The Cancer Cell Line Encyclopedia enables predictive modelling of anticancer drug sensitivity. Nature. 2012;483(7391):603-7. Epub 2012/03/31. doi: 10.1038/nature11003. PubMed PMID: 22460905; PMCID: PMC3320027.
40. Obenauf AC, Zou Y, Ji AL, Vanharanta S, Shu W, Shi H, et al. Therapy-induced tumour secretomes promote resistance and tumour progression. Nature. 2015;520(7547):368-72. Epub 2015/03/26. doi: 10.1038/nature14336. PubMed PMID: 25807485; PMCID: PMC4507807.
41. Zheng X, Han H, Liu GP, Ma YX, Pan RL, Sang LJ, et al. LncRNA wires up Hippo and Hedgehog signaling to reprogramme glucose metabolism. Embo j. 2017;36(22):3325-35. Epub 2017/10/01. doi: 10.15252/embj.201797609. PubMed PMID: 28963395; PMCID: PMC5686550.

42. Nicolas FJ, Hill CS. Attenuation of the TGF-beta-Smad signaling pathway in pancreatic tumor cells confers resistance to TGF-beta-induced growth arrest. Oncogene. 2003;22(24):3698-711. Epub 2003/06/13. doi: 10.1038/sj.onc.1206420. PubMed PMID: 12802277.
43. Liu X, Zhang SM, McGeary MK, Krykbaeva I, Lai L, Jansen DJ, et al. KDM5B Promotes Drug Resistance by Regulating Melanoma-Propagating Cell Subpopulations. Mol Cancer Ther. 2019;18(3):706-17. Epub 2018/12/14. doi: 10.1158/1535-7163.Mct-18-0395. PubMed PMID: 30523048; PMCID: PMC6397704.
44. Ablain J, Xu M, Rothschild H, Jordan RC, Mito JK, Daniels BH, et al. Human tumor genomics and zebrafish modeling identify SPRED1 loss as a driver of mucosal melanoma. Science. 2018;362(6418):1055-60. Epub 2018/11/06. doi: 10.1126/science.aau6509. PubMed PMID: 30385465.
45. Ndoye A, Budina-Kolomets A, Kugel CH, 3rd, Webster MR, Kaur A, Behera R, et al. ATG5 Mediates a Positive Feedback Loop between Wnt Signaling and Autophagy in Melanoma. Cancer research. 2017;77(21):5873-85. Epub 2017/09/10. doi: 10.1158/0008-5472.Can-17-0907. PubMed PMID: 28887323; PMCID: PMC5718045.
46. Kim Y, Yeon M, Jeoung D. DDX53 Regulates Cancer Stem Cell-Like Properties by Binding to SOX-2. Mol Cells. 2017;40(5):322-30. Epub 2017/05/26. doi: 10.14348/molcells.2017.0001. PubMed PMID: 28535666; PMCID: PMC5463040.
47. White RM, Zon LI. Melanocytes in development, regeneration, and cancer. Cell Stem Cell. 2008;3(3):242-52. Epub 2008/09/13. doi: 10.1016/j.stem.2008.08.005. PubMed PMID: 18786412.
48. Webster MR, Fane ME, Alicea GM, Basu S, Kossenkov AV, Marino GE, et al. Paradoxical Role for Wild-Type p53 in Driving Therapy Resistance in Melanoma. Molecular Cell. 2020;77(3):633-44.e5.
49. Shao DD, Xue W, Krall EB, Bhutkar A, Piccioni F, Wang X, et al. KRAS and YAP1 converge to regulate EMT and tumor survival. Cell. 2014;158(1):171-84. Epub 2014/06/24. doi: 10.1016/j.cell.2014.06.004. PubMed PMID: 24954536; PMCID: PMC4110062.
50. Lin L, Sabnis AJ, Chan E, Olivas V, Cade L, Pazarentzos E, et al. The Hippo effector YAP promotes resistance to RAF- and MEK-targeted cancer therapies. Nat Genet. 2015;47(3):250-6. Epub 2015/02/09. doi: 10.1038/ng.3218. PubMed PMID: 25665005.
51. White RM, Cech J, Ratanasirintrawoot S, Lin CY, Rahl PB, Burke CJ, et al. DHODH modulates transcriptional elongation in the neural crest and melanoma. Nature. 2011;471(7339):518-22. Epub 2011/03/25. doi: 10.1038/nature09882. PubMed PMID: 21430780; PMCID: PMC3759979.
52. Hecht JH, Weiner JA, Post SR, Chun J. Ventricular zone gene-1 (vzg-1) encodes a lysophosphatidic acid receptor expressed in neurogenic regions of the developing cerebral cortex. J Cell Biol. 1996;135(4):1071-83. Epub 1996/11/01. PubMed PMID: 8922387; PMCID: PMC2133395.
53. Contos JJ, Fukushima N, Weiner JA, Kaushal D, Chun J. Requirement for the lpA1 lysophosphatidic acid receptor gene in normal suckling behavior. Proc Natl Acad Sci U S A. 2000;97(24):13384-9. Epub 2000/11/23. doi: 10.1073/pnas.97.24.13384. PubMed PMID: 11087877; PMCID: PMC27233.
54. Muinonen-Martin AJ, Susanto O, Zhang Q, Smethurst E, Faller WJ, Veltman DM, et al. Melanoma cells break down LPA to establish local gradients that drive chemotactic dispersal. PLoS biology. 2014;12(10):e1001966. Epub 2014/10/15. doi: 10.1371/journal.pbio.1001966. PubMed PMID: 25313567; PMCID: PMC4196730.
55. Susanto O, Koh YWH, Morrice N, Tumanov S, Thomason PA, Nielson M, et al. LPP3 mediates self-generation of chemotactic LPA gradients by melanoma cells. Journal of cell science. 2017;130(20):3455-66. Epub 2017/09/06. doi: 10.1242/jcs.207514. PubMed PMID: 28871044; PMCID: PMC5665449.
56. Gloerich M, Bos JL. Regulating Rap small G-proteins in time and space. Trends Cell Biol. 2011;21(10):615-23. Epub 2011/08/09. doi: 10.1016/j.tcb.2011.07.001. PubMed PMID: 21820312.

57. Cui R, Cao G, Bai H, Zhang Z. LPAR1 regulates the development of intratumoral heterogeneity in ovarian serous cystadenocarcinoma by activating the PI3K/AKT signaling pathway. Cancer cell international. 2019;19:201. Epub 2019/08/07. doi: 10.1186/s12935-019-0920-0. PubMed PMID: 31384176; PMCID: PMC6664705.
58. Hawes BE, Luttrell LM, van Biesen T, Lefkowitz RJ. Phosphatidylinositol 3-kinase is an early intermediate in the G beta gamma-mediated mitogen-activated protein kinase signaling pathway. J Biol Chem. 1996;271(21):12133-6. Epub 1996/05/24. PubMed PMID: 8647803.
59. van Biesen T, Hawes BE, Luttrell DK, Krueger KM, Touhara K, Porfiri E, et al. Receptor-tyrosine-kinase- and G beta gamma-mediated MAP kinase activation by a common signalling pathway. Nature. 1995;376(6543):781-4. Epub 1995/08/31. doi: 10.1038/376781a0. PubMed PMID: 7651538.
60. Gopal YN, Rizos H, Chen G, Deng W, Frederick DT, Cooper ZA, et al. Inhibition of mTORC1/2 overcomes resistance to MAPK pathway inhibitors mediated by PGC1alpha and oxidative phosphorylation in melanoma. Cancer Res. 2014;74(23):7037-47. Epub 2014/10/10. doi: 10.1158/0008-5472.Can-14-1392. PubMed PMID: 25297634; PMCID: PMC4347853.
61. Fisher ML, Grun D, Adhikary G, Xu W, Eckert RL. Inhibition of YAP function overcomes BRAF inhibitor resistance in melanoma cancer stem cells. Oncotarget. 2017;8(66):110257-72. Epub 2018/01/05. doi: 10.18632/oncotarget.22628. PubMed PMID: 29299145; PMCID: PMC5746380.
62. Hugo W, Shi H, Sun L, Piva M, Song C, Kong X, et al. Non-genomic and Immune Evolution of Melanoma Acquiring MAPKi Resistance. Cell. 2015;162(6):1271-85. doi: 10.1016/j.cell.2015.07.061. PubMed PMID: 26359985.

FIGURE LEGENDS

Figure 1. Transcriptome juxtaposition and targeted screens identify LPAR1. (**A**) Volcano plot for genes selected from RNAseq and microarray data. Highlighted are best novel genes enriched in melanoma and NCLSC cultures relative to melanocytes by fold change and adjusted pvalue (for RNA-seq: $p<10^{-10}$ or fold>4, for microarrays: $p<10^{-6}$ or fold>4). (**B**) Scatter plot showing the averaged results of the targeted siRNA screen in 1205Lu and WM1366 cells. The X-axis represents the normalized growth and the Y-axis represents each individual gene from 1-253. Four individual siRNAs against each gene were used. The blue dots represent the siEIF4A3 and the green dots represent non-specific siRNAs as negative control. (**C**) The top 30 genes identified in the primary screen were used for the secondary screen. (**D**) Ingenuity pathway analysis of the top 30 genes in the screen identifies the LPAR1-RAP1A axis as the most significant network among the gene candidates. (**E**) Relative gene expression levels of LPAR1 in melanoma, NCLSC and melanocytes assayed by qRT-PCR. Biological replicates (n=3) for each condition are included.

Figure 2. LPAR1 promotes melanoma and NCLSC survival. (**A**) 1205Lu, WM9, WM989 and WM983B cells were seeded in 6-well plates, serum-starved for 24 hr and then treated with LPA (10 μM, 0 – 72 hr). Cell numbers were quantified for LPA or vehicle treated cells (n=3, Student's T-test, * $p<0.05$, error bars indicate SD). (**B**) Melanoma cells, melanocytes and fibroblasts were transfected with control siNS or siLPAR1 and incubated for 96 hr, followed by the cell proliferation MTT assay. n=3; * $p<0.05$, all statistics compared proliferation between siNS or siLPAR1 for each respective cell line. (**C**) Melanoma cells were infected with lentiviral constructs expressing control shNS or shLPAR1 and grown for 3 weeks. Cells were stained with Crystal Violet; n=3.

Figure 3. LPAR1 drives melanoma motility and invasiveness. (**A**) A wound healing assay was performed in WM9 cells with the knockdown of LPAR1. Red lines indicate the leading edges of migrating cells. Scale bar, 50 μm. The percentage of wound closure after different time periods of migration was calculated and shown Error bars, SD; n = 3; * $p < 0.05$. (**B**) Transwell migration assay (without matrigel coating) was performed for WM9 cells infected with luciferase shRNA (shLuc) or shLPAR1. Scale bar,100 μM. The number of migrated cells were quantified to the right. Error bars are SD; n = 3; * $p < 0.05$. (**C**)Transwell invasion assay (with matrigel coating) was performed in 1205Lu cells infected with shLuc or shLPAR1. Scale bar, 100 μM. The numbers of invaded cells were quantified. Error bars, SD; n = 3; * $p < 0.05$. (**D**) 1205Lu cells transfected with siNS or siLPAR1 were used to make skin reconstructs. S100, green; DAPI, blue. Scale bar for H&E staining, 50 μM. Scale bar for immunofluorescence staining, 20 μM.

Figure 4. LPA regulates LPAR1 signaling through a RAPGEF5-RAP1A-axis. (**A**) MTT assay was performed in WM9 LPAR1 knockdown cells as well as in LPAR1 knockdown cells with the expression of RAP1A (Q63E, constitutively active mutant), RAP1A (S17N, inactive mutant), overexpression of RAP1A (wt) or RAPGEF5. n=3; ANOVA with post-hoc Holm-Sidak's multiple comparisons test were applied. * Holm-Sidak's multiple comparisons adjusted $p<0.05$; error bars indicate SD. (**B**) GST-tagged RalGDS-RBD was conjugated on glutathione Sepharose 4B and incubated with WM9 cells infected with shLuc, shLPAR1-1 or shLPAR1-2. (**C-D**) GSTtagged RalGDS-RBD was conjugated on glutathione Sepharose 4B and incubated with WM9 cells with the addition of LPA followed by the knockdown of RAPGEF5 (**C**) or the overexpression of RAPGEF5 followed by the knockdown of LPAR1 (D). (**E**) Melanoma cell lines were transfected with siNS, siRAPGEF5 or siRAP1A and grown for 3 weeks in long-term colony formation assays. Cells were subsequently stained with crystal violet and imaged, n=3. ANOVA with post-hoc Holm-Sidak's multiple comparisons test were applied. * Holm-Sidak's multiple comparisons adjusted $p<0.05$; error bars indicate SD. (**F**) Transwell invasion assay (with matrigel coating) was performed in WM9 cell lines infected with shNS, shRAPGEF5 or shRAP1A. (**G**) WM9 cells transfected with siNS, siRAPGEF5, or siRAP1A were used to make skin reconstructs. S100, green; DAPI, blue. Scale bar for H&E staining, 50 μM. Scale bar for immunofluorescence staining, 20 μM.

Figure 5. mTOR and YAP are downstream effectors of the LPAR1-axis. (**A**) WM9 cells were transfected with siNS or siLPAR1 for 48 hr. Protein lysate was analyzed by RPPA. Shown are the proteins most significantly altered. (**B**) A panel of $LPAR1^{lo}$ and $LPAR1^{hi}$ melanoma cell lines were transfected with siNS or siLPAR1 for 48 hr. Protein lysate was immunoblotted to validate findings in (**A**). (**C**) Immunostaining of YAP in WM9 cells transfected with siNS or siLPAR1 using an anti-YAP antibody (green); nuclei were stained with DAPI (blue). The ratio of YAP localized to the nucleus was quantified and shown to the right. (**D**) WM9 cells expressing shNS, shYAP, shS6K, shYAP+shS6K, or shLPAR1 were grown for 3 weeks in long-term colony formation assays and subsequently stained with crystal violet. An unpaired two-tailed t-test was used for all studies.

Figure 6. LPAR1 promotes intrinsic- and acquired-resistance to targeted therapy. (**A**) A scatterplot was generated to examine the correlation between LPAR1 and MITF, as well as the correlation between LPAR1 and AXL using gene expression data in the TCGA. A line of best fit is shown. (**B**) Relative gene expression levels of LPAR1 were assessed by quantitative PCR in a panel of paired melanoma cell lines that were therapy naïve, or developed acquired resistance to BRAF inhibition or combination BRAF/MEK

inhibition. n=3; ANOVA with post-hoc Holm-Sidak's multiple comparisons test were applied. * Holm-Sidak's multiple comparisons adjusted p<0.05. (**C**) Melanoma cells were transfected with siNS or siLPAR1 for 96 hr, followed by the cell proliferation MTT assay, n=3. ANOVA with post-hoc Holm-Sidak's multiple comparisons test were applied. * Holm-Sidak's multiple comparisons adjusted p<0.05. (**D**) UACC903 and UACC903CR cells were transfected with siNS or siLPAR1 for 48 hr. Lysate was analyzed by RPPA and shown are the proteins most significantly altered in UACC903CR ($LPAR1^{hi}$) versus parental UACC903 ($LPAR1^{lo}$) cells. (**E**) Western blotting validation of lysate from UACC903, UACC903BR and UACC903CR cells treated as in (**D**). (**F**) Immunohistochemistry for LPAR1 staining in patient-derived tissue. Quantification of 61 tissues is shown to the right, LPAR1 staining is red. Fisher's exact test was used to compare % tissue samples by the LPAR1 staining level. (**G**) Tumor volumes from WM9 xenografts infected with lentiviral constructs expressing shCon or shLPAR1 were treated with vehicle control or PLX4032 (25 mg/kg/d, chow). * p<0.05. n=10 mice/arm. The tumors in the shLPAR1 + BRAFi arm are statistically smaller than all other arms. The tumors in the shControl + BRAFi arm and the shLPAR1 arm are both statistically smaller than the tumors in the shControl arm. (**H**) Schematic illustration of LPAR1 expression fluctuation with differentiation status of melanoma cells. Under targeted therapy, $LPAR1^{lo}$ cells undergo dedifferentiation to a $LPAR1^{hi}$, NCSC-like state that is resistant to targeted therapy via elevated LPAR1->RAPGEF5->RAP1A->mTOR/YAP activity. An unpaired two-tailed t-test was used for two group comparisons, unless otherwise stated.

Author Manuscript Published OnlineFirst on August 30, 2021; DOI: 10.1158/0008-5472.CAN-20-1496
Author manuscripts have been peer reviewed and accepted for publication but have not yet been edited.

Figure 1

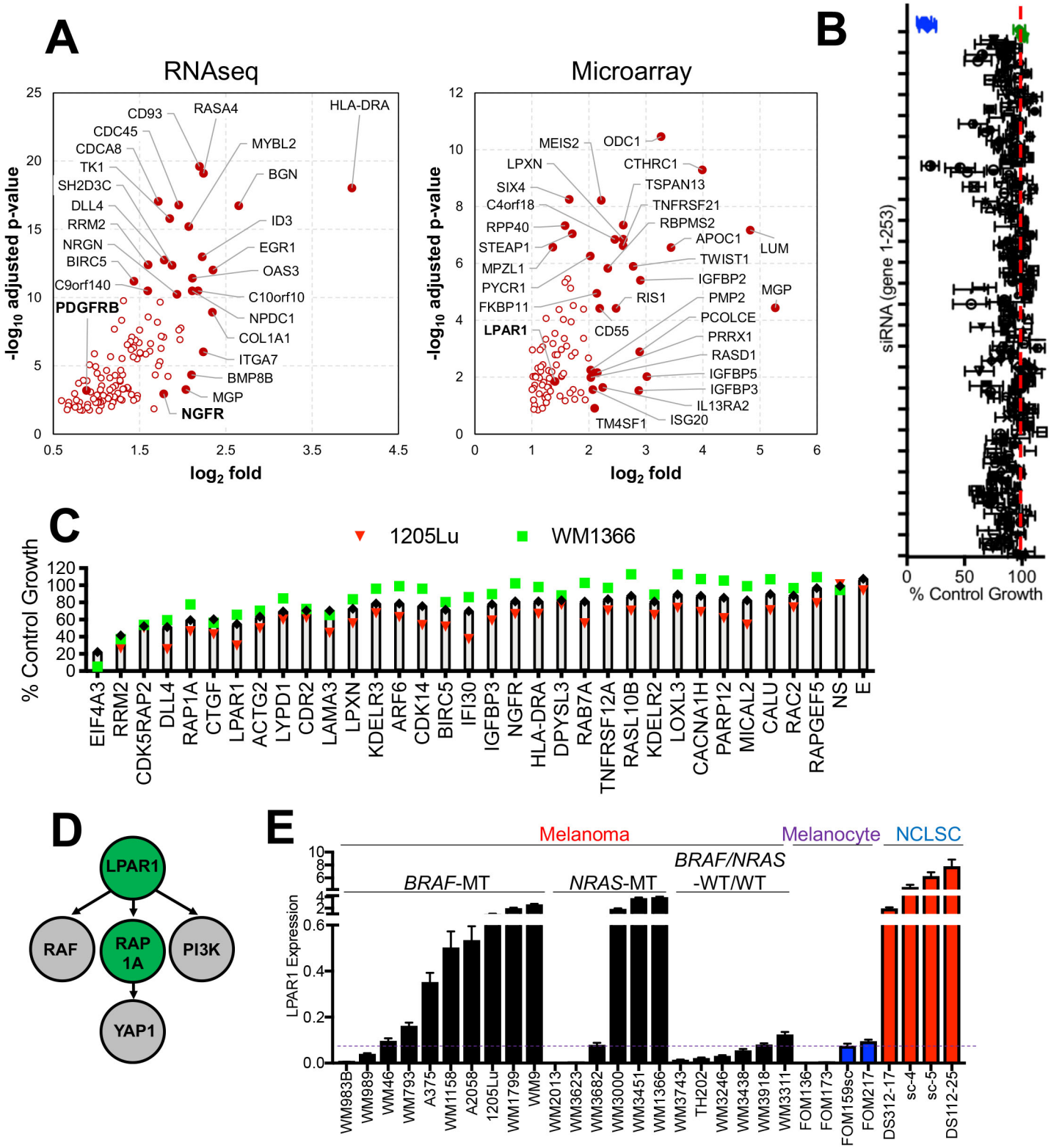

Author Manuscript Published OnlineFirst on August 30, 2021; DOI: 10.1158/0008-5472.CAN-20-1496
Author manuscripts have been peer reviewed and accepted for publication but have not yet been edited.

Figure 2

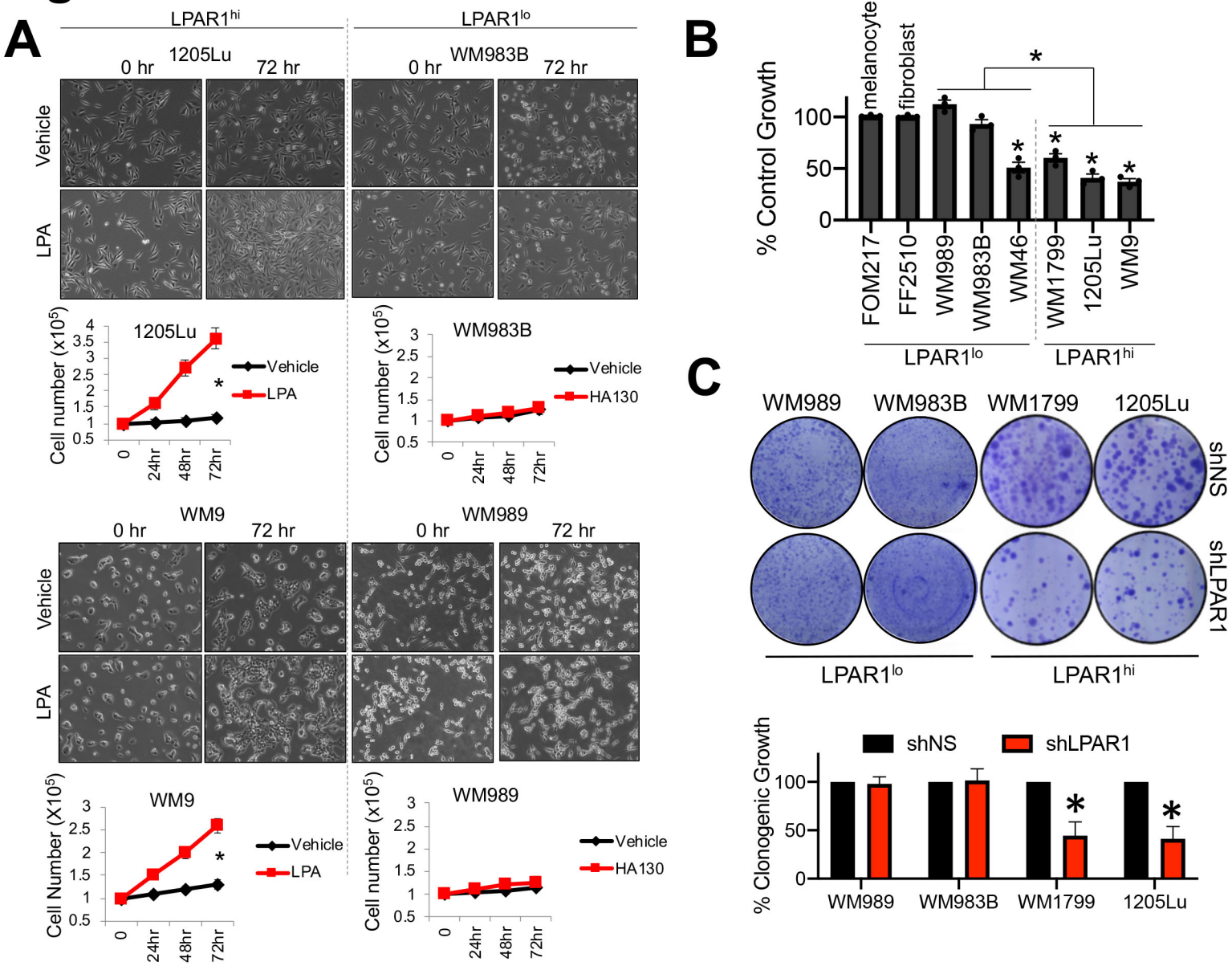

Figure 3

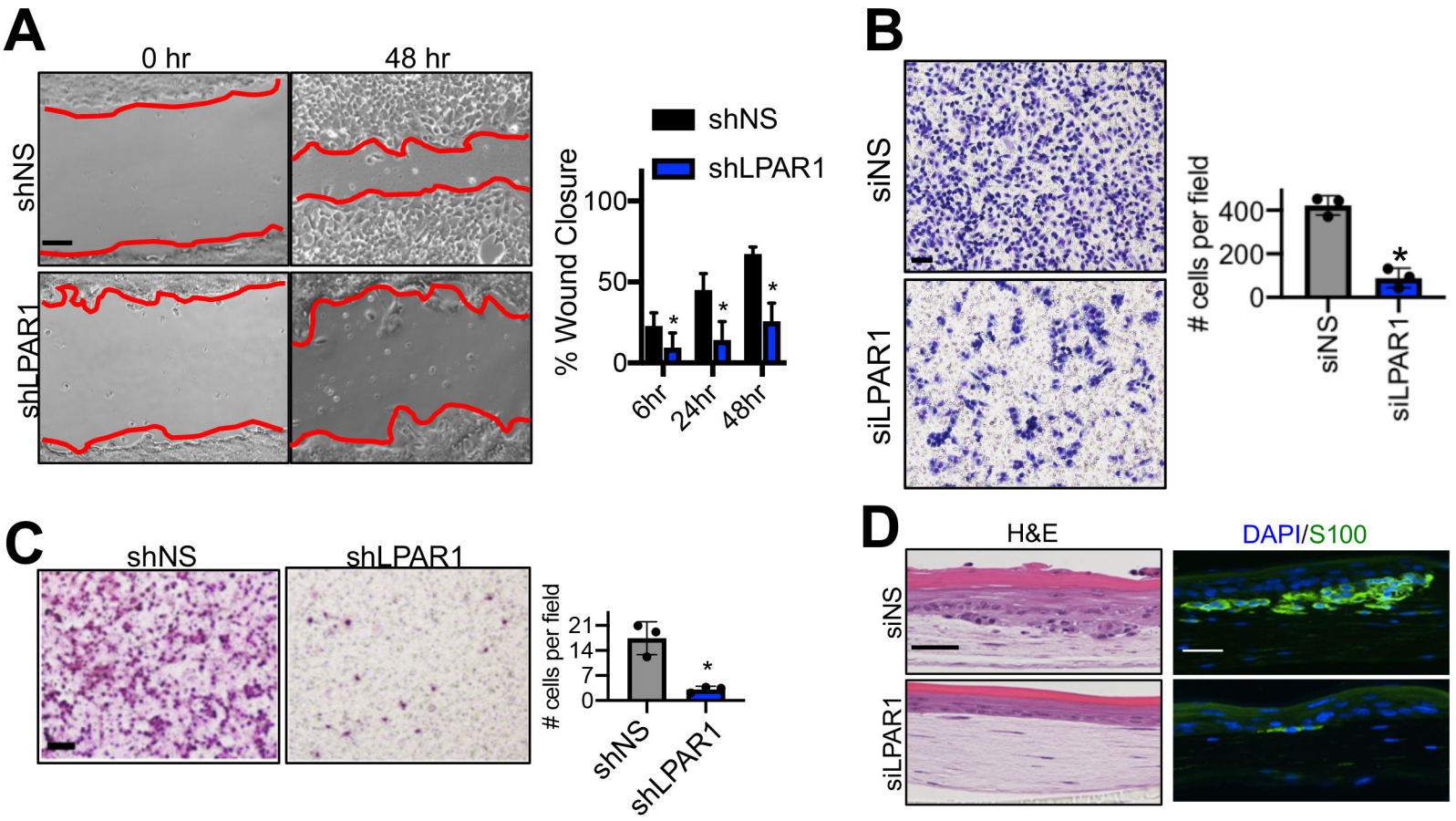

Figure 4

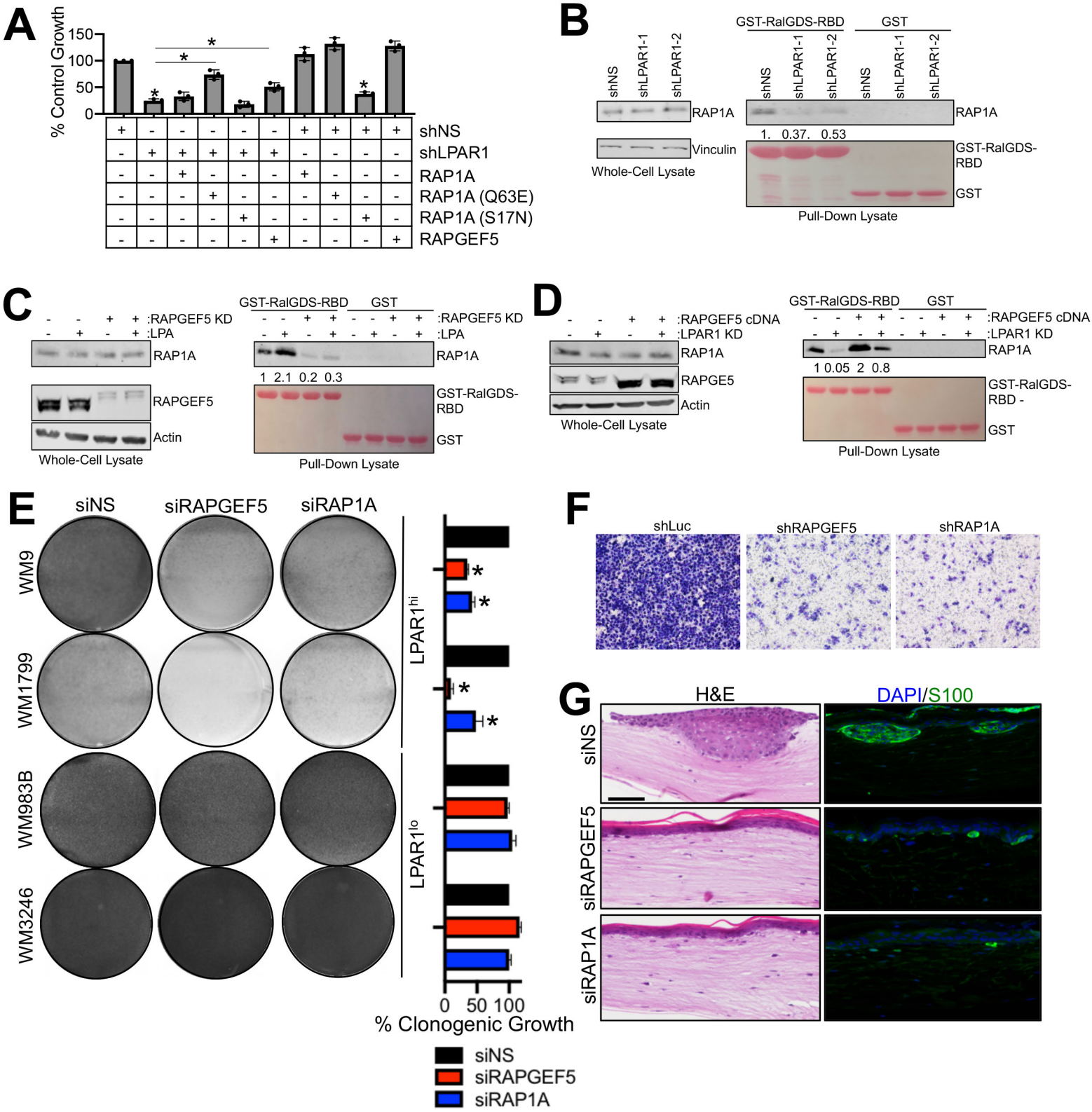

Figure 5

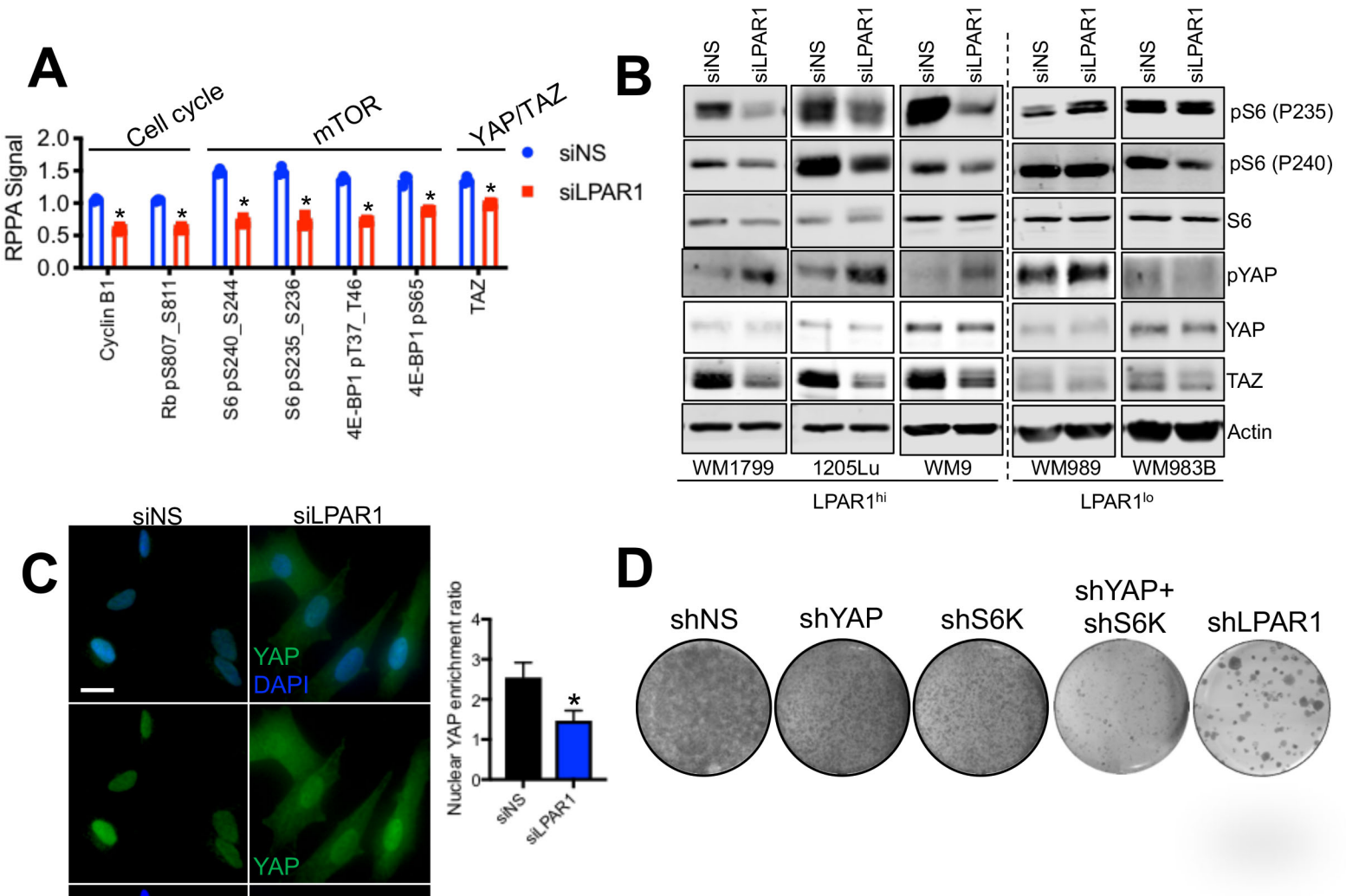

Figure 6

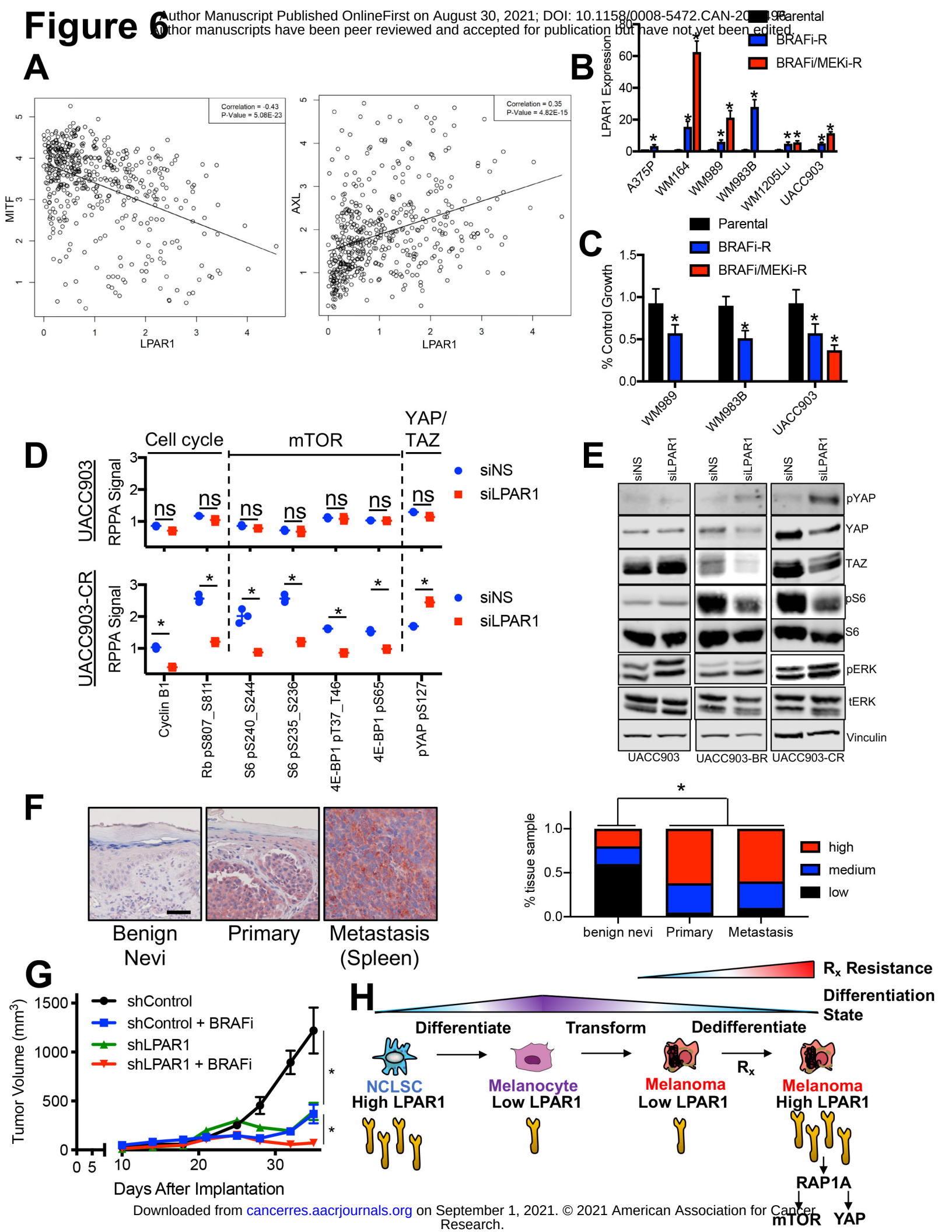

AACR American Association for Cancer Research

Cancer Research

The Journal of Cancer Research (1916–1930) | The American Journal of Cancer (1931–1940)

Neural crest-like stem cell transcriptome analysis identifies LPAR1 in melanoma progression and therapy resistance.

Jianglan Liu, Vito W. Rebecca, Andrew V. Kossenkov, et al.

Cancer Res Published OnlineFirst August 30, 2021.